Interferometric Measurement of the Biphoton Wave Function

Federica A. Beduini,[1,*] Joanna A. Zielińska,[1] Vito G. Lucivero,[1] Yannick A. de Icaza Astiz,[1] and Morgan W. Mitchell[2]
[1]ICFO-Institut de Ciencies Fotoniques, Avinguda Carl Friedrich Gauss, 3, 08860 Castelldefels, Barcelona, Spain
[2]ICREA-Institució Catalana de Recerca i Estudis Avançats, 08015 Barcelona, Spain
(Received 25 July 2014; published 31 October 2014)

Interference between an unknown two-photon state (a "biphoton") and the two-photon component of a reference state gives a phase-sensitive arrival-time distribution containing full information about the biphoton temporal wave function. Using a coherent state as a reference, we observe this interference and reconstruct the wave function of single-mode biphotons from a low-intensity narrow band squeezed vacuum state.

DOI: 10.1103/PhysRevLett.113.183602 PACS numbers: 42.50.Ar, 42.50.Dv, 42.50.St

Introduction.—Correlated photon pairs, or "biphotons," are a paradigmatic experimental system in quantum technology, with applications in quantum communications [1], quantum information processing [2], foundations of physics [3], and quantum metrology [4]. In many experiments, the performance of a biphoton source is closely tied to the two-photon wave function (TPWF) that describes the temporal correlations of the photons. For example, the visibility of Hong-Ou-Mandel interference depends on the TPWF, even when some other degree of freedom, e.g., polarization, is used to encode quantum information [5]. Measurements of the TPWF are also used to characterize realistic photon pair sources, allowing the diagnosis of experimental defects, e.g., imperfect poling in the down-conversion crystal [6] or dispersion [7].

The TPWF $\psi(t_1, t_2)$ is an intrinsically multidimensional object, depending on the two time coordinates t_1 and t_2 [8]. Methods to characterize the TPWF include measurement of the joint spectral density [9], measurement of the joint temporal density [6], nonclassical interference using the Hong-Ou-Mandel effect [10–12], and nonlinear optical processes [7,13–15]. All of these techniques give partial information about the TPWF. For example, the joint temporal density gives the magnitude $|\psi(t_1, t_2)|$, while the joint spectral density gives the magnitude of Fourier components.

Full measurement of the TPWF requires a phase-sensitive and tomographic measurement, applied to a continuous range of time values. Some elements of this approach have been demonstrated: Quantum state tomography [16] has been widely used to characterize aggregate measures of a quantum state, e.g., the integrated field of a pulse, or the mode describing a single frequency component. This includes traditional homodyne methods using strong local oscillators [16] and mesoscopic methods using weak local oscillators plus photon-counting detection [17]. Homodyne [18,19] and polychromatic heterodyne [20] characterization of a single photon wave function has also been reported.

Here we demonstrate full characterization of a two-photon wave function, based on the phenomenon of interference of two-photon amplitudes [21–23]. A similar method is proposed in Ref. [24]. Our approach combines the use of a weak phase reference and photon counting detection as in Ref. [17] with wave-function detection over an extended time span as in Refs. [18,19], and adds the new elements of time-correlated photon counting, as required by the dimensionality of the TPWF. We demonstrate the method by reconstructing the TPWF of single-mode squeezed vacuum from a subthreshold optical parametric oscillator (OPO) or in single-photon terms, degenerate cavity-enhanced spontaneous parametric down-conversion (SPDC). An attractive feature of our approach is a very direct data interpretation, without the ill-posed inverse problem typically encountered in tomography.

One- and two-photon wave functions.—We use field correlation functions [25] to characterize optical quantum states. For a state $|\lambda\rangle$, the so-called "one-photon wave function" is $\psi_i^{(\lambda)}(t) \equiv \langle 0|E_i^{(+)}(t)|\lambda\rangle$, where $E_i^{(+)}(t)$ is the positive-frequency part of the electric field operator for mode i. Because $E_i^{(+)}(t)$ removes one photon, this represents $|\lambda\rangle$ projected onto the one-photon subspace. Similarly, the "two-photon wave function" is [10]

$$\psi_{i,j}^{(\lambda)}(t_1, t_2) \equiv \langle 0|E_i^{(+)}(t_1)E_j^{(+)}(t_2)|\lambda\rangle. \quad (1)$$

As with Schrödinger wave functions, neither $\psi_i^{(\lambda)}(t)$ nor $\psi_{i,j}^{(\lambda)}(t_1, t_2)$ is directly observable. On the other hand, the second-order intensity correlation function

$$g_{ij}^{(2)}(t_1, t_2) \propto \langle \lambda|E_j^{(-)}(t_2)E_i^{(-)}(t_1)E_i^{(+)}(t_1)E_j^{(+)}(t_2)|\lambda\rangle \quad (2)$$

is directly observable in photon pair arrival time distributions. In the commonly encountered case that $|\lambda\rangle$ contains no more than two photons, this is proportional to $|\psi_{ij}^{(\lambda)}(t_1, t_2)|^2$. The second order correlation function then gives important but incomplete information about the two-photon wave function, as it contains no information on the phase of $\psi_{ij}^{(\lambda)}$, which is a complex function.

Coherent state reference.—We consider a scenario in which $|\lambda\rangle$ occupies one propagating mode (V), while a time-independent coherent state $|\alpha\rangle$ occupies an ancilla mode (H). We measure the correlation function

$$\tilde{\psi}^{(\kappa)}_{AB}(t_1,t_2) = \langle 0|\tilde{E}^{(+)}_A(t_1)\tilde{E}^{(+)}_B(t_2)|\kappa\rangle \tag{3}$$

of the global state $|\kappa\rangle = |\lambda\rangle \otimes |\alpha\rangle$ with a polarimeter setup, as shown in Fig. 1: a quarter- and a half-wave plate apply a unitary transformation on the polarization, then a beam displacer separates the two polarization components, so that the field operator associated with detector $A(B)$ is

$$\tilde{E}^{(+)}_A(t) = \cos\theta E^{(+)}_H(t) + e^{i\phi}\sin\theta E^{(+)}_V(t), \tag{4}$$

$$\tilde{E}^{(+)}_B(t) = e^{-i\phi}\sin\theta E^{(+)}_H(t) - \cos\theta E^{(+)}_V(t), \tag{5}$$

where θ and ϕ are the polar and azimuthal angle in the Bloch sphere, respectively.

The two-photon wave function of the global state becomes then

$$\begin{aligned}\tilde{\psi}^{(\kappa)}_{AB}(t_1,t_2) = {} & e^{-i\phi}\cos\theta\sin\theta\psi^{(\alpha)}_{HH}\langle 0|\lambda\rangle \\ & - e^{i\phi}\cos\theta\sin\theta\psi^{(\lambda)}_{VV}(t_1,t_2)\langle 0|\alpha\rangle \\ & + \sin^2\theta\psi^{(\lambda)}_{V}(t_1)\psi^{(\alpha)}_{H}(t_2) - \cos^2\theta\psi^{(\alpha)}_{H}(t_1)\psi^{(\lambda)}_{V}(t_2).\end{aligned} \tag{6}$$

The last two terms in Eq. (6) vanish, because $\psi^{(\lambda)}_V(t) \equiv \langle 0|E^{(+)}_V(t)|\lambda\rangle = 0$ when $|\lambda\rangle$ is squeezed vacuum. More generally, $\psi^{(\lambda)}_V(t)$ vanishes for any state invariant under $E^{(+)}_V(t) \to -E^{(+)}_V(t)$ or equivalently $a_V(\omega) \to a_V(\omega)\exp[i\pi]$. The symmetry of the down-conversion Hamiltonian $H \propto \chi^{(2)} a^\dagger_V a^\dagger_V a_p + \text{H.c.}$, and of dephasing and decoherence processes, guarantees $\psi^{(\lambda)}_V(t) = 0$ in the broad class of experiments using spontaneous, i.e., vacuum-driven, down-conversion.

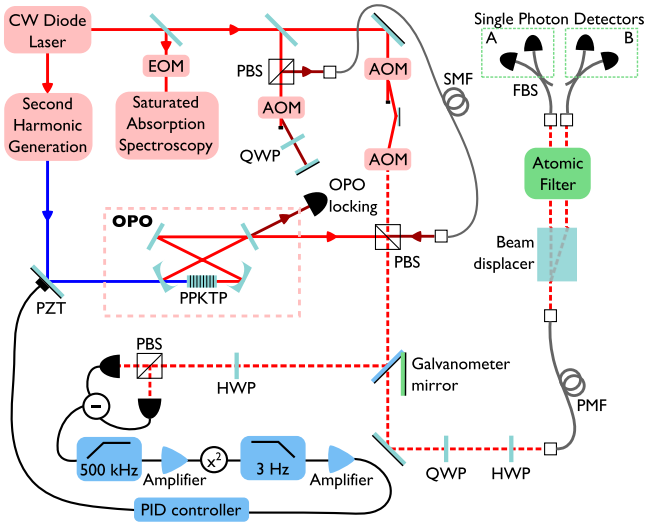

FIG. 1 (color online). Experimental setup. AOM (EOM): acousto- (electro-) optic modulator. PBS: polarizing beam splitter. QWP (HWP): quarter- (half-)wave plate. PZT: piezoelectric actuator. SMF: single mode fiber. PMF: polarization maintaining fiber. FBS: fiber beam splitter.

Taking $\theta = \pi/4$ for simplicity, we can write the measurable second order correlation function as

$$g^{(2)}_{AB(\kappa)}(t_1,t_2) \propto |\gamma e^{-2i\phi} - \psi^{(\lambda)}_{VV}(t_1,t_2)|^2, \tag{7}$$

where $\gamma = \psi^{(\alpha)}_{HH}\langle 0|\lambda\rangle\langle 0|\alpha\rangle^{-1}$. We note that now $g^{(2)}_{AB(\kappa)}$, which is directly measurable, contains information about the phase of $\psi^{(\lambda)}_{VV}(t_1,t_2)$, through interference against $|\alpha\rangle$. For convenience, we choose the phase origin so that α, and thus γ, is real, and as indicated already $\theta = \pi/4$. To find $\psi^{(\lambda)}_{VV}$, it is convenient to measure with the azimuthal angle $\phi = k\pi/3$, $k = \{0,1,2\}$, i.e., symmetrically placed within the period of $\exp[2i\phi]$. We denote the resulting $g^{(2)}$ values as y_k.

It is then possible to solve Eq. (7) to obtain the TPWF

$$\psi^{(\lambda)}_{VV} = \mathring{y}/\gamma, \tag{8}$$

$$\gamma = \frac{1}{\sqrt{2}}\sqrt{\bar{y} + \sqrt{3\bar{y}^2 - 2\overline{y^2}}}, \tag{9}$$

where $\mathring{y} \equiv -\sum_{k=0}^{2} y_k \exp[-ik2\pi/3]/3$, $\bar{y} \equiv (y_0+y_1+y_2)/3$ and $\overline{y^2} \equiv (y_0^2+y_1^2+y_2^2)/3$, keeping in mind that $\psi^{(\lambda)}_{VV}$, the y_k and γ all depend on (t_1,t_2).

As with other coincidence-based measurements [1–4], losses do not affect the reconstruction results: they only imply longer acquisition time in order to reach statistical significance.

Experimental realization.—To test the technique, we measure the two-photon wave function of weakly squeezed vacuum from a subthreshold degenerate OPO. A continuous-wave diode laser at 794.7 nm generates both the coherent reference beam and, after being amplified and doubled in frequency, a 397.4 nm pump beam for the OPO, described in Ref. [26], which generates a vertically polarized (V) squeezed vacuum state via SPDC in a periodically poled Potassium titanyl phosphate (PPKTP) crystal. The cavity length is actively stabilized with a Pound-Drever-Hall lock, to keep one longitudinal V mode resonant at the laser frequency. The locking beam is H polarized, counterpropagating, and shifted in frequency by an acousto-optic modulator (AOM), to match the frequency of an H-polarized mode. The AOM rf power is chopped and the detectors are electronically gated: coincidence data are acquired only when the locking light is off. With these measures, the

contribution of locking light to the accidental coincidences background is minimized.

The V-polarized squeezed vacuum is combined with the H-polarized coherent reference at a polarizing beam splitter to generate a beam with copropagating squeezed and reference components. The polarization transformation of Eqs. (4) and (5) is implemented with a quarter- and a half-wave plate, and the beam is coupled into a polarization maintaining fiber, with its fast axis aligned to H polarization when $\theta = \phi = 0$. At the fiber output, the two polarization components are separated into parallel beams by a calcite beam displacer and passed through a narrow band (445 MHz) atomic filter [27,28], in order to isolate the squeezed vacuum and block with high efficiency the hundreds of nondegenerate frequency modes generated by the OPO. The maximum transmission frequency of this filter is located at 2.7 GHz to the red of the center of the rubidium D_1 line, and the laser frequency is stabilized at this particular frequency by using an integrated electro-optic modulator to add sidebands to the laser prior to the saturated absorption spectroscopy. Each filtered beam is then coupled into a single-mode fiber and split with a 50/50 fiber beam splitter into a pair of single-photon counting avalanche photo diodes. A time-of-flight recorder time stamps each arrival and correlations are computed on a PC.

A low OPO pump power (1 mW, 0.4% of threshold) is used so that contributions of more than two photons are negligible. The coherent reference power is chosen to give a similar rate of two-photon events, for high visibility interference.

The relative phase ϕ_{rel} between the coherent and the squeezed beam is stabilized by a quantum noise lock: One Stokes component is detected with a balanced polarimeter, and the noise power in a 3 Hz bandwidth above 500 kHz is computed analogically using a multiplier circuit. This signal is fed back by a servo loop to a piezoelectric actuator on a mirror in the pump path, to stabilize the pump phase by a side-of-fringe lock. A galvanometer mirror is used to switch between the single-photon counting and stabilization setups at a frequency of ~100 Hz. The reference beam power is increased during the stabilization part of the cycle, to reach the shot-noise-limited regime optimal for detection of the squeezing and operation of the noise lock. Two cascaded AOMs, whose rf power is chopped synchronously with the galvanometer mirror, modulate the coherent reference beam power, so that it has high power when the light is entering the stabilization setup and low power when the photon counting part is active. The system can maintain a fixed ϕ_{rel} over several hours.

Results.—As our light source is continuous wave, the light statistics are stationary: the correlations and wave function depend only on the photon arrival-time difference $\tau = t_1 - t_2$. We compute the experimental $g^{(2)}_{AB(\kappa)}(\tau)$ from coincidences between detector groups A and B in Fig. 1, with a 4 ns coincidence window, a compromise between temporal resolution and statistical significance.

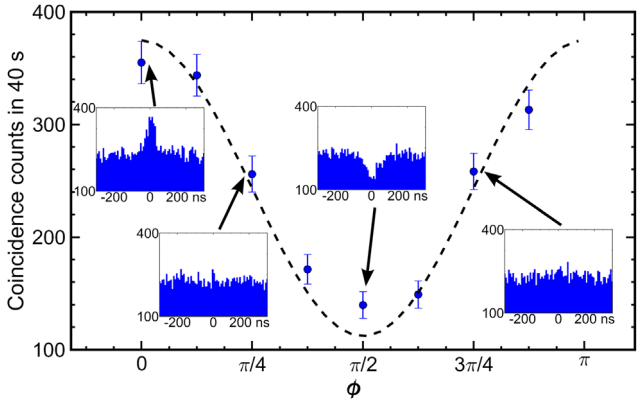

FIG. 2 (color online). Arrival-time distributions showing interference of two-photon amplitudes. Main graph shows coincidence rates $g^{(2)}_{AB(\kappa)}(0)$ (circles) for delay $\tau = 0$ versus analysis phase ϕ for a coincidence windows of 8 ns. The dashed line is $A[1 + V\cos(2\phi)]$, where $V = 0.54$ is the expected visibility and A comes from a fit to the data. The sinusoidal behavior in good agreement with the data reveals two-photon interference as predicted by Eq. (7). Error bars show $\pm 1\sigma$ (standard deviation) statistical uncertainty, assuming Poisson statistics. Insets show $g^{(2)}_{AB(\kappa)}(\tau)$ for the values of ϕ indicated with arrows. These clearly show the passage from constructive interference at $\phi = 0$, where a peak is visible, to destructive interference at $\phi = \pi/2$, where a dip appears.

As shown in Fig. 2, we observe both constructive and destructive interference, e.g., at $\phi = 0$ and $\phi = \pi/2$, respectively. The observation of a dip in the correlation function is especially interesting, because it clearly signals destructive interference of two-photon amplitudes from the coherent and the squeezed vacuum states. The interference visibility is limited by accidental coincidence counts, which are mainly due to the residual OPO locking beam and to nondegenerate modes passing through the filter [28]. However, these do not affect the wave-function reconstruction: the accidentals add a term independent from τ to the $g^{(2)}$, which is canceled by the subtractions in Eq. (8). Also unbalance between the pair rates of the coherent and the squeezed vacuum states reduces the visibility [see Eq. (7)], without affecting the reconstruction: for the data shown in Fig. 2, this implies an expected visibility of 0.54, after subtraction of the accidental counts, in agreement with observations.

We next collect $g^{(2)}_{AB(\kappa)}(\tau)$ data for $\phi = 0, \pi/3, 2\pi/3$ and use Eqs. (8) and (9) to reconstruct $\psi^{(\lambda)}_{VV}(\tau)$, shown in Fig. 3. The reconstruction is direct: $\psi^{(\lambda)}_{VV}$ at a given τ depends only on coincidence events at that value of τ. The results are consistent with a double-exponential amplitude with 26 ns full width at half maximum (FWHM), as expected for a squeezed vacuum state from an OPO with the 8.1 MHz

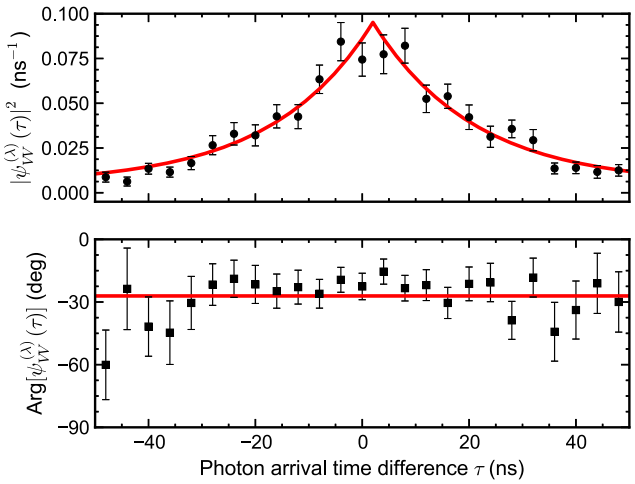

FIG. 3 (color online). Squared amplitude (above) and phase (below) of the reconstructed two-photon wave function for the squeezed vacuum state. The solid line shows the predicted, double exponential amplitude describing an ideal squeezed vacuum state from our OPO with an independently measured 8.1 MHz bandwidth, with the amplitude and the offset fitted to the data. Error bars show $\pm 1\sigma$ statistical uncertainty assuming Poisson statistics and using propagation of error through Eqs. (8) and (9).

FWHM bandwidth independently measured on our system. The phase of $\psi_{VV}^{(\lambda)}$, consistent with a nonzero constant value, is reconstructed with a statistical uncertainty that decreases with increasing $|\psi_{VV}^{(\lambda)}|$, reaching $\sigma_\phi \approx \pm 6$ degree near $\tau = 0$. A constant phase is expected for an ideal OPO, while a phase defect could signal cavity or crystal imperfections [6,7]. The phase offset is tunable via the side-of-fringe lock that sets the relative phase of the squeezed vacuum and reference, and is another indication of interference at the two-photon level.

Our state can be assumed pure. We measure fluctuations of a few degrees in the phase stabilization and a few percent in the pump amplitude, the sources of mixedness in the two-photon component of the squeezed state. In simulations, when the reconstruction procedure is applied to the resulting mixed state, the result agrees with the statistically averaged ψ_{VV} precisely in phase, and to within 4% in amplitude. This is below the statistical uncertainties shown in Fig. 3.

Conclusion.—We have demonstrated complete measurement of the complex temporal wave function of biphotons using interference of the two-photon amplitude against a reference. The interference gives a phase-sensitive arrival-time distribution, from which we reconstruct the biphoton wave function. In contrast to most tomographic procedures [5,16], only three measurement settings are required to find the real and imaginary parts of the wave function, as well as the strength of the reference state. The inverse problem is thus neither overdetermined nor underdetermined, and can be solved analytically. We analyze the output of a narrowband, atom-resonant OPO operating at 795 nm, and find results in good agreement with theory. The technique works because SPDC, including the squeezer we use, produces superpositions containing both two- and zero-photon parts. When combined with a coherent state, also a superposition containing both two-and zero-photon parts, two indistinguishable paths to any given coincidence event coexist and interfere. This clearly shows interference of two-photon amplitudes from distinct sources. The technique could be used to detect and correct errors in quantum light sources for quantum information processing [29] and quantum metrology [30], or to match the output of multiple sources for quantum communications [31].

We thank F. Wolfgramm and F. Martin Ciurana for helpful discussions. This work was supported by the Spanish MINECO project MAGO (Ref. FIS2011-23520), European Research Council project AQUMET and by Fundació Privada CELLEX. J. Z. was supported by the FI-DGR PhD-fellowship program of the Generalitat of Catalonia. Y. A. de I. A. was supported by the scholarship BES-2009-017461, under project FIS2007-60179.

*federica.beduini@icfo.es

[1] C.-Z. Peng, T. Yang, X.-H. Bao, J. Zhang, X.-M. Jin, F.-Y. Feng, B. Yang, J. Yang, J. Yin, Q. Zhang, N. Li, B.-L. Tian, and J.-W. Pan, Phys. Rev. Lett. **94**, 150501 (2005).
[2] P. Walther, K. J. Resch, T. Rudolph, E. Schenck, H. Weinfurter, V. Vedral, M. Aspelmeyer, and A. Zeilinger, Nature (London) **434**, 169 (2005).
[3] M. Giustina, A. Mech, S. Ramelow, B. Wittmann, J. Kofler, J. Beyer, A. Lita, B. Calkins, T. Gerrits, S. W. Nam, R. Ursin, and A. Zeilinger, Nature (London) **497**, 227 (2013).
[4] M. W. Mitchell, J. S. Lundeen, and A. M. Steinberg, Nature (London) **429**, 161 (2004).
[5] R. B. A. Adamson, L. K. Shalm, M. W. Mitchell, and A. M. Steinberg, Phys. Rev. Lett. **98**, 043601 (2007).
[6] O. Kuzucu, F. N. C. Wong, S. Kurimura, and S. Tovstonog, Phys. Rev. Lett. **101**, 153602 (2008).
[7] K. A. O'Donnell and A. B. U'Ren, Phys. Rev. Lett. **103**, 123602 (2009).
[8] A. Valencia, A. Ceré, X. Shi, G. Molina-Terriza, and J. P. Torres, Phys. Rev. Lett. **99**, 243601 (2007).
[9] P. J. Mosley, J. S. Lundeen, B. J. Smith, P. Wasylczyk, A. B. U'Ren, C. Silberhorn, and I. A. Walmsley, Phys. Rev. Lett. **100**, 133601 (2008).
[10] A. Sergienko, Y. Shih, and M. Rubin, J. Opt. Soc. Am. B **12**, 859 (1995).
[11] V. Giovannetti, L. Maccone, J. H. Shapiro, and F. N. C. Wong, Phys. Rev. A **66**, 043813 (2002).
[12] R. Okamoto, S. Takeuchi, and K. Sasaki, Phys. Rev. A **74**, 011801 (2006).
[13] B. Dayan, A. Pe'er, A. A. Friesem, and Y. Silberberg, Phys. Rev. Lett. **93**, 023005 (2004).
[14] A. Pe'er, B. Dayan, A. A. Friesem, and Y. Silberberg, Phys. Rev. Lett. **94**, 073601 (2005).

[15] S. Sensarn, I. Ali-Khan, G. Y. Yin, and S. E. Harris, Phys. Rev. Lett. **102**, 053602 (2009).
[16] D. T. Smithey, M. Beck, M. G. Raymer, and A. Faridani, Phys. Rev. Lett. **70**, 1244 (1993).
[17] G. Puentes, J. S. Lundeen, M. P. A. Branderhorst, H. B. Coldenstrodt-Ronge, B. J. Smith, and I. A. Walmsley, Phys. Rev. Lett. **102**, 080404 (2009).
[18] J. S. Neergaard-Nielsen, B. M. Nielsen, C. Hettich, K. Mølmer, and E. S. Polzik, Phys. Rev. Lett. **97**, 083604 (2006).
[19] O. Morin, C. Fabre, and J. Laurat, Phys. Rev. Lett. **111**, 213602 (2013).
[20] Z. Qin, A. S. Prasad, T. Brannan, A. MacRae, A. Lezama, and A. I. Lvovsky, arXiv:1405.6251.
[21] J. R. Torgerson and L. Mandel, J. Opt. Soc. Am. B **14**, 2417 (1997).
[22] Y. J. Lu and Z. Y. Ou, Phys. Rev. Lett. **88**, 023601 (2001).
[23] T. Douce, A. Eckstein, S. P. Walborn, A. Z. Khoury, S. Ducci, A. Keller, T. Coudreau, and P. Milman, Sci. Rep. **3**, 3530 (2013).
[24] C. Ren and H. F. Hofmann, Phys. Rev. A **86**, 043823 (2012).
[25] R. J. Glauber, Phys. Rev. **130**, 2529 (1963).
[26] A. Predojević, Z. Zhai, J. M. Caballero, and M. W. Mitchell, Phys. Rev. A **78**, 063820 (2008).
[27] J. A. Zielińska, F. A. Beduini, N. Godbout, and M. W. Mitchell, Opt. Lett. **37**, 524 (2012).
[28] J. A. Zielińska, F. A. Beduini, V. G. Lucivero, and M. W. Mitchell, Opt. Express.**22**, 25307 (2014).
[29] F. Wolfgramm, X. Xing, A. Ceré, A. Predojević, A. M. Steinberg, and M. W. Mitchell, Opt. Express **16**, 18145 (2008).
[30] F. Wolfgramm, C. Vitelli, F. A. Beduini, N. Godbout, and M. W. Mitchell, Nat. Photonics **7**, 28 (2013).
[31] J. Fekete, D. Rieländer, M. Cristiani, and H. de Riedmatten, Phys. Rev. Lett. **110**, 220502 (2013).